

XPS Photoelectron Profilography

G..Mladenov, K.Vutova, T.Tanaka* and K.Kawabata*

Institute of electronics, Bulg. Acad. of Sciences, Sofia 1784, Tzarigr. shose 72 ,Bulgaria

**Dept.of electronics, Hiroshima Instit.of Technol., 211, Miyake, Saikiku, Hiroshima7315193, Japan*

(Received October 7 1998; accepted December 22 1998)

Mathematical modeling of the angular distribution of the X-ray generated photoelectron signal is described. Surface roughness models, corresponding algorithms and obtained results are presented. A conclusion for the mean slope angle value of surface roughness structures of the studied sample is made. The developed technique for evaluation of integral characteristics of surface roughness is appropriate for studying the surface structures with a height bigger than the photoelectron ejection depth. The results are significant also at analysis of electron spectra, generated from textured surfaces.

1. Introduction

At analysis of electron spectra (XPS, AES), generated from a textured surface, usually is accepted a smooth surface, which can involve mistakes at the interpretation of some measured data, namely angle resolved spectra. The surface roughness effect on the electron spectra have been discussed [1-7] and contradictory conclusions are made.

Mathematical model for calculation of the photoelectron angular distribution, generated by X-ray irradiation of a textured surface are presented in this paper. The used approximations support understanding the shape and features of the measured photoelectron angle distributions. A comparison between calculated XPS and the experimentally measured angle-resolved XPS is shown.

2. Model description

For investigation of the surface topology effect on XPS angular distribution, it is convenient to assume that the sample surface consists of many repeating simple geometrical structures.

Cones with equal base diameter and height is assumed to model a roughness structures. They are located in statistical manner on the studied surface in a direct touch or the distance between them is small. The value of this separation is in the range of $[0, \delta]$, that is a small part of R . A single cone, shaping roughness peak and the angle definitions are shown in Fig.1. The angle α is the slope angle of an inclined small surface

element dS from the side wall of the observed surface roughness structure (α is measured between dS and xOy plane, coincides with the base wall). In this case, α is also the angle between the side wall and the base wall of the cone. The angle θ is the tilting angle of investigated sample realized by inclination of the sample holder. This angle is the argument of XPS angular distributions of the sample (the cone axis correspond to $\theta = 0$).

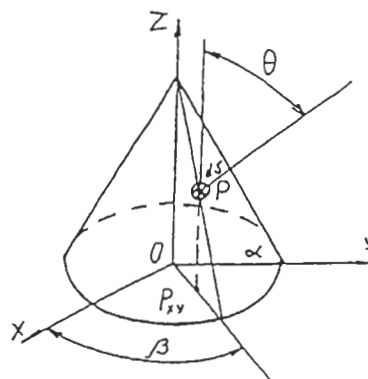


Figure 1. Illustration of a conical shaped roughness peak, coordinates and angles.

The generated photoelectron intensity from a thick sample of uniform material composition, with a flat (no textured, smooth) surface, assuming a straight-line trajectory of ejected photoelectrons is given by cos law. In the case of textured surface, the XPS intensity is a sum of signals from every type of side wall inclinations, at which one can divide the side

walls of the assumed roughness peaks (accounting the sign of α and type of roughness peak in the case of a multi-shape or multi-dimension peaks structures). The total photoelectron signal assembles the photoelectrons, ejected from such selected areas of the roughness peaks walls.

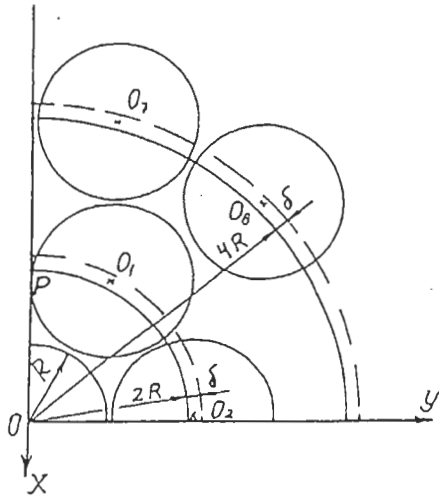


Figure 2. Bird's-eye view of peaks in conical roughness model.

In the case of assumed model (using one type shaped roughness structure with the axial-symmetry of the peaks - Fig.1, Fig.2) the total XPS signal, emitted in a small solid angle $d\Omega$, around the direction θ , consists of the signals from two type surfaces. They can obtaine, when divide the surface by a plane of symmetry, determined by the tilting axis x and the peak axis of symmetry. Then the XPS intensity can be expressed as:

$$I(\theta) = \int_S I_1 K_{sh1}(\theta) k_1(\theta - \alpha) \cos(\theta - \alpha) k_{\beta 1} \cos\beta ds + \int_S I_2 K_{sh2}(\theta) k_2(\theta + \alpha) \cos(\theta + \alpha) k_{\beta 2} \cos\beta ds, \quad (1)$$

where: I_1, I_2 are normalization photoelectron intensity constants; $k_n(\theta \pm \alpha)$ and k_β are coefficients, accounted the shielding of the ejected photoelectrons from the adjacent sample surface. The angle β is the angle between Ox and OP_{xy} (Fig.1). The coefficients K_{sh1} and K_{sh2} characterize the shadowing effect of ejected photoelectrons from the adjacent roughness peaks. Their values can be described as:

$K_{sh1} = 1$ in the range: $\alpha - \pi/2 < \theta < \theta_{max}$, and $K_{sh2} = 1$ in the range: $\pi/2 - \alpha > \theta > -\theta_{max}$, and $K_{sh1} = K_{sh2} = 0$ at values of θ out of these ranges. The average angle of shielding photoelectrons from adjacent roughness peaks θ_{max} is determined by:

$\theta_{max} = \text{arctg} \{ [(z_{top} - z_p)_{aver} - z_p] / (2R - r_p) \}$, (2) where z_{top} is the highest z -coordinate of the shielding top line, z_p is the z -coordinate of dS , $r_p = OP_{xy}$, $2R$ is the cone base diameter (Fig.1,3). The average is done in all the β and in eq. (2) is included only the first shielding term from the top shielding line at $2R$ circle (Fig.2).

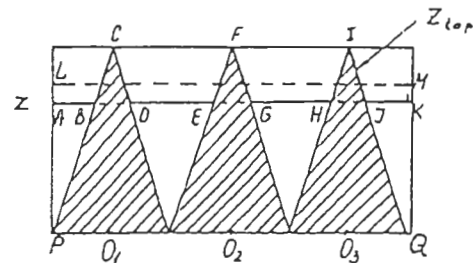


Figure 3. Shield screen model.

3. Results and discussions.

3.1 Model of triangular prisms and rings

A similar model uses triangular prisms to approximate the sample surface [5-7]. Calculations of angular distributions of the ejected photoelectrons were done at different angles α (between side and base walls of the prisms). Calculated angular distributions of XPS intensity at $\alpha = 30^\circ$ are shown in Fig.4.

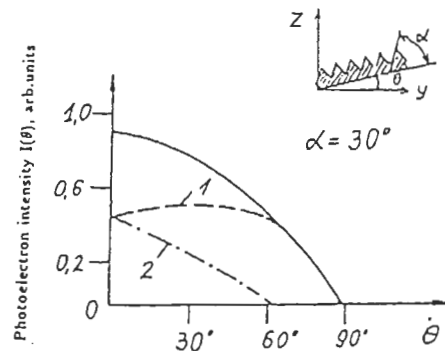


Figure 4. Calculation results, using triangular prisms model at $\alpha = 30^\circ$.

The XPS intensity is symmetrical to axis $\theta=0^\circ$, i.e. to the spectrometer vertical axis. The solid curve presents the photoelectron angular distribution from the total sample surface. The shadowing effect is taken into account and it shapes the dispersal. The maximum of the components of this distribution, originated from two types of side walls are at $\theta=-\alpha$ and $\theta=\alpha$ (the curves 1 and 2 correspond to the terms, containing $\cos(\theta+\alpha)$ and $\cos(\theta-\alpha)$, respectively). Due to the shadowing effect at big values of θ , XPS intensity of the real sample is lowered much before $(\theta-\alpha) = \pi / 2$. The solid curve is an amount of the intensities 1 and 2, and it is similar to cos-distribution, but it is not a result of cos law. At small values of θ it is a sum of two cos shaped curves, and its rest part takes into account the linearly decreased shadowing probability. The photoelectrons, traveling ahead of longest ejection distances and originating from shallow depths, are in the middle region of this distribution, and are not at its end, which is a difference from the expected result by cos law.

Obtained results, using the model of triangular rings (generated by the rotation of a triangular wave around an axis) on the sample surface are in a good agreement with the data in [2].

3.2 Roughness peaks model using cones.

This model is described in section 2. Fig.5 shows three curves, representing the results for cones at different values of α (curve 1 - at $\alpha=30^\circ$, curve 2 - at $\alpha=60^\circ$, curve 3 - at $\alpha=70^\circ$).

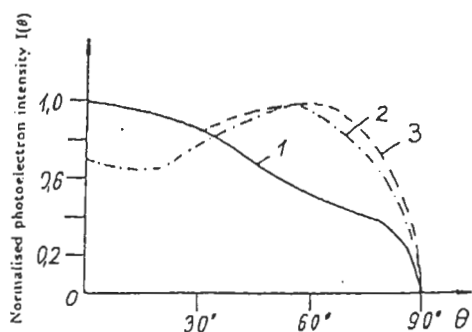


Figure 5. The normalised photoelectron intensity as a function of the angle θ , in the case of conical model.

In the calculations is assumed that the values of θ_m is the same for slim segments of side cone wall, due to the averaging of the shielding situation at many side walls of different cones. The differences in the values of $(\theta \pm \alpha)$ or in the distances between the ejecting segment pixels and the shielding screen (adjacent cone), at different values of β , are neglected, due to the existence of maximum of emitted photoelectrons in the direction of θ . The difference between distributions, represented by curves 1 and 2, starts at $\theta = \pi / 2 - 60^\circ = 30^\circ$. The increase of the photoelectron intensity, shown with curve 3, starts at $\theta = \pi / 2 - 70^\circ = 20^\circ$. The maximums of the distributions (due to a more transparent shield) at $\alpha=60^\circ$ and $\alpha=70^\circ$ - curves 2 and 3 (Fig.5) are not observed in the cases of previous models (section 3.1).

3.3 Model using surface roughness peaks shaped as hemispheres

In this model the peaks distribution on the studied surface is the same, as in the conical model (Fig.2). But this model uses hemispheres to approximate the surface roughness. The distance between a shadowing shield and an ejecting pixel is assumed a constant. Slim segments, for which θ_{max} is the same, are used. The summation of the ejected electrons (eq. (1)) is carry out from all the segments, instead of summarizing the shadowing coefficients for all the side walls (at given α and θ) and then multiplying them by cos law. The calculated photoelectron distribution is shown in Fig. 6.

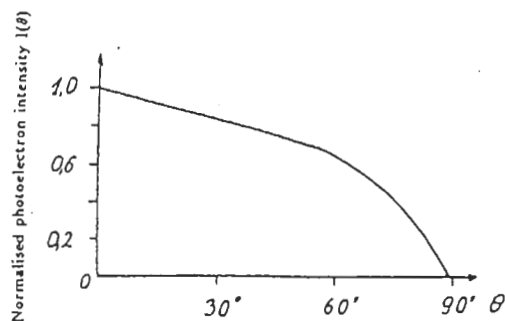


Figure 6. Normalised XPS intensity distribution, using the model of hemispherical surface roughness peaks.

3.4 Remark about photoelectron collector.

A narrow photoelectron collector is accepted in these calculations. In [6] is shown that when we use wide collector (or collecting the XPS by a bigger solid angle, for example 30°-45°), the calculated curves are more smooth, without a change of the shown curve character.

3.5 Comparison with experimental result.

Fig.7 shows a comparison between the XPS angular distributions, experimentally measured [8] (curve 2) and calculated, using the model 3.2, at a slope $\alpha = 30^\circ$ (curve 1). It can be seen an enough good coincidence. It means, that the the slope angle value of the side walls of the surface roughness structures is near to 30° .

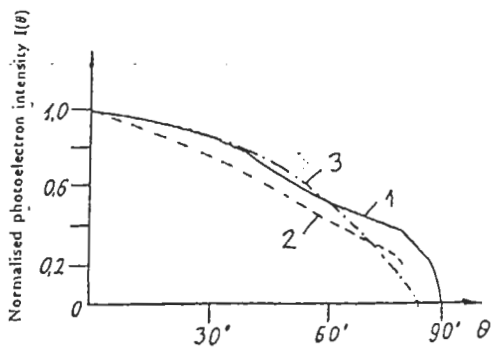


Figure 7. Comparison between calculated data - curve 1 (conical model, $\alpha = 30^\circ$) and experimental data - curve 2. Curve 3 presents calculated data, using the model of triangular prisms.

For example, in Fig.8 is shown a profile, measured by **AFM** profilometer of the SnO₂ sample.

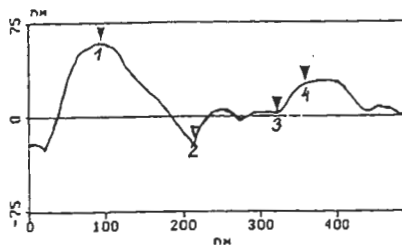


Figure 8. Scan line profile of SnO₂.

4. Conclusions

In this paper we describe models, using different geometrical shapes and cos law of X-ray photoelectron ejection (this mean that the height of the roughness structures is 3-5 times higher than the ejected depth [9]) for calculation of the XPS angular intensity distribution. From comparisons between experimentally measured and calculated XPS distributions, one can estimate the value of the mean angle of surface roughness structures. In this paper calculations are done for four surface models. A reasonable good coincidence is observed, when an experimentally measured XPS distribution for SnO₂ sample (investigated in [8]) is compared with calculated XPS data (using conical peaks model). The used model is acceptable for this sample and the evaluation of the mean slope sample angle is near to 30° .

5. Acknowledgment

The authors (G.M and K.V) gratefully acknowledge the financial support of the Hiroshima Institute of Technology .

6. References

[1] C.S.Fadley and al., J.Electr.Spectr.Rel. Phenom., 4, 93 (1974).
 [2] L.Bernardez and al, Surf.Sci.139,541(1984).
 [3] P.Gunter and al, Appl.Surf.Sci.115, 342(1997)
 [4] P.Zalm, Surf.Interf.Anal.26, 352 (1998).
 [5] K.Kawabata and al., Jap.Journ. of Appl.Phys, 30, 7-8, L1231 , (1991).
 [6] K.Vutova, G.Mladenov, K.Kawabata and T.Tanaka, Proc. of the Nat.Conference with Intern. participation "Electronika'98", Botevgrad, Publ. UEEB, Oct.1998,36(1998).
 [7] K.Vutova, T.Tanaka, K.Kawabata and G.Mladenov, , Abstract Book, 14th International Vacuum Congress, Birmingham,31 August- 4 Sept. 1998, 52 (1998).
 [8] K.Vutova, G.Mladenov, T.Tanaka and K.Kawabata , Proceed.of the Nat.Conference with Intern. Participation "Electronika'98", Botevgrad, Publ. UEEB, Oct.1998,29(1998).
 [9] D.R.Penn, Journ.Electron Spectr. and Rel.Phenomena, 9, 29, (1976).